NVV auger spectra from W(100)

S. P. Withrow,[a] P. E. Luscher,[b] and F. M. Propst[c]

Coordinated Science Laboratory, University of Illinois, Urbana, Illinois 61801

W. H. Weinberg[d]

Department of Chemistry and Chemical Engineering, California Institute of Technology, Pasadena, California 91125

(Received 19 September 1977; accepted 2 January 1978)

The *NVV* Auger spectrum from a clean W(100) surface has been measured in the second derivative, $d^2N(E)/dE^2$, mode to enhance fine structure. This measurement is compared with spectra generated from both the self-convolution of the tungsten valence-band bulk density of states (obtained from a relativistic APW energy band calculation) and a "restricted convolution" in which only transitions involving electrons from the same valence energy are allowed. The restricted convolution for a model of the Auger process in which both N_6VV and N_7VV transitions contribute offers the best match of theory and experiment. No distinct evidence of Auger emission involving the surface resonance present on W(100) is observed. Effects of H_2 and O_2 adsorption on the Auger spectrum of the W(100) surface are reported.

PACS numbers: 79.20.Fv, 82.65.My, 71.25.Pi

The energy distributions of electrons emitted from solid surfaces following core-valence-valence (*CVV*) Auger transitions contain considerable information on the electronic structure of the solid. For materials in which electron transition and escape probabilities are constant across the valence band and the effects of background, inelastic loses, and final states can be adequately assessed, the electron bulk density of valence-band states (BDOS) may be obtained from a deconvolution of the *CVV* Auger spectrum. While this procedure has been successfully applied to some materials,[1] difficulties often encountered in satisfying the above criteria limit its use. Conversely, if the BDOS is known, its self-convolution can be compared to the *CVV* Auger spectrum to study the nature of the interactions involved in the Auger process. This approach was first proposed by Lander[2] and its application has provided evidence for the contribution to the Auger line shape of such electronic processes as final state effects and transition probabilities.[3–10]

Using a model for the *CVV* Auger process in which all possible "up" and "down" transitions are assumed equally probable, the distribution in energy of emitted Auger electrons, $S(E)$, is given by

$$S(E) = \sum_C M_C[E_C - \phi - \Delta E - A(\xi) * A(\xi)] \qquad (1)$$

where E_{CBE} is the binding energy of the core electrons measured from the Fermi level, E_F, and ϕ is the work function. $A(\xi)*A(\xi)$ represents the self-convolution of $A(\xi)$ which is the density of valence-band states times a constant transition factor. It is assumed that final state and relaxation screening effects can be approximated by shifting the spectrum in energy by ΔE. In practice ΔE is a constant which is empirically chosen to fit the data. The factor M_C is the electron population of the core level and the summation represents contributions to $S(E)$ from transitions involving different core levels.

Eq. (1) is not valid when the assumption of equal probability for all possible transitions breaks down. In fact, we have been unable to find a satisfactory correlation between our Auger spectra and that calculated on the basis of a self-convolution of the valence-band BDOS, i.e., using Eq. (1). We find, however, that good agreement can be obtained with a model in which all "up and down" transitions are equally probable but with the restriction that both electrons involved in an Auger transition originate at the same valence energy. This model effectively describes Auger spectra in which structure arising from cross terms between different energy states within the valence band is weak. For this model the Auger electron energy distribution is given by

$$D(E) = \sum_C M_C[E_C - \phi - \Delta E - A(\xi/2)] \qquad (2)$$

where $A(\xi/2)$ represents the "restricted" convolution.

In this paper we report the results of an investigation of *NVV* Auger emission from a W(100) surface. In order to resolve fine structure in the electron energy distribution, $N(E)$, the spectra have been taken in the second derivative, $d^2N(E)/dE^2$, mode. We compare these measurements to the second derivative of Auger spectra predicted from a relativistic augmented plane wave (RAPW) BDOS calculation for tungsten[11] using models for the Auger process involving both one and two core levels. Recently Avery published experimental results for *NVV* transitions in tungsten in which he attributes all of the structure to N_7VV and N_7-surface state-surface state, $N_{7\mathcal{A}\mathcal{A}}$, transitions.[10] We present an alternative explanation of the Auger spectrum which includes both N_6VV and N_7VV processes but no surface state. The effects of hydrogen and oxygen adsorption on the *NVV* spectra are also presented.

EXPERIMENTAL

The Auger measurements presented in this paper were obtained using a double-pass electrostatic deflection analyzer

which is a part of a UHV multiple technique surface analysis system.[12] Pulse counting was used for acquisition of $N(E)$ while synchronous detection techniques were used in obtaining $N(E)$ and its first and second derivatives. In addition to improving the sensitivity to fine structure in the spectra, the use of the second energy derivative is particularly advantageous for these studies since it provides second order background suppression and because peaks in $N(E)$ result in peaks in $-d^2N(E)/dE^2$ (written $N''(E)$ in the following sections for convenience).

The incident electron beam was provided by an electron gun located internal to and coaxial with the analyzer. In taking spectra, primary beam energies, E_p, between ~100 eV and 115 eV at a current of 5 μA incident normal to the W(100) surface were used. The analyzer accepts electrons scattered from the sample at polar angles of 35° ± 2.5°. Energy distributions were obtained by fixing the analyzer pass energy at 10 eV and decelerating the scattered electron signal using grids located in front of the analyzer. The energy resolution for the analyzer for the conditions of 10-eV pass energy and 0.5-eV modulation voltage for synchronous detection was approximately 0.75 eV.

The experimental sample was a tungsten disk cut from a single crystal supplied by the Materials Research Corporation and mechanically and electrochemically polished on both sides to within 0.1° of the (100) orientation.[13] Its final dimensions were 0.8 cm in diameter and 0.33 mm thick. The sample was spotwelded to a 0.18 mm diameter tungsten wire support which was 9.5 mm long. This wire was spotwelded to the end of a manipulator which positioned the sample and provided for electrical and thermal control. Temperatures were measured using a W vs W-26% Re thermocouple spotwelded to the edge of the sample.[14]

Initially, the tungsten sample was heated at 2200 K in 1×10^{-9} Torr (1.3×10^{-7} Pa) of oxygen for 9 h to remove carbon. Following this cleaning procedure, a surface free of contamination could be produced routinely by heating to greater than 2200 K for 30 s. The Auger sensitivity was approximately 1% of a monolayer for carbon and oxygen. Hydrogen impurity was monitored by ELS,[15] LEED, and ESD and estimated from all three techniques to be less than 2% of a monolayer. The LEED pattern was as expected for a clean, well-defined W(100) surface.

Base pressure in the UHV system was below 9.3×10^{-9} Pa (7×10^{-11} Torr). Gas dosing was accomplished using a collimated molecular beam source. During dosing the system pressure as read on the Bayard-Alpert gauge never rose above 1.3×10^{-8} Pa.

RESULTS

The electron energy distribution, N(E), and its second derivative, $d^2N(E)/dE^2$, obtained from clean W(100) at a primary beam energy, E_p, of 99.5 eV are shown in Fig. 1. All of the structure above 50 eV results from characteristic energy loss mechanisms.[16,17] Prominent among these excitations are the W $4f_{5/2}$ (N_{VI}) and $4f_{7/2}$ (N_{VII}) core ionizations at loss energies, w, of 32.4 and 34.6 eV below the elastic peak. Radiationless recombination of valence band electrons to these

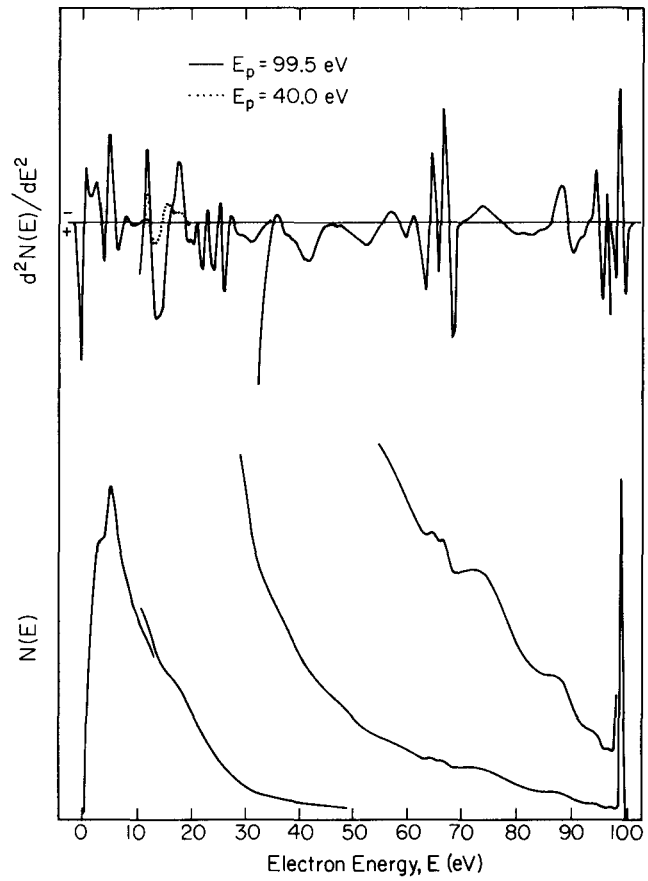

FIG. 1. $N(E)$ and $d^2N(E)/dE^2$ for a primary energy of 99.5 eV. The modulation voltage for the second derivative was 1 V peak to peak. Different regions of the spectra are shown at different amplifications.

ionized cores leads to the emission of *NVV* Auger electrons.

All of the structure observed in Fig. 1 below 50 eV is true secondary fine structure and results from modulation of the secondary electron cascade by the energy band structure and from electrons emitted via the Auger process. The marked suppression in positive $d^2N(E)/dE^2$ of the slowly varying components of the true secondary cascade is obvious. Comparison of the fine structure peaks below approximately 12 eV with the RAPW band structure calculations of Christensen and Feuerbacher[11] shows a correlation with the conduction band BDOS. The shoulder in $N(E)$ at 3.5 eV corresponds with the major forbidden gap in the BDOS calculations which has also been observed as extinction in the UPS data of Feuerbacher and Christensen.[18] *VVV* Auger emission is possible out to 4.5 eV. The secondary peaks at E = 36.2 and 46.5 eV are often observed in published Auger spectra.[19] Only the $5p_{1/2}$ (O_{II}) core orbital at a binding energy of $\simeq$47 eV[20] can produce structure at these energies through Auger processes. However, it is not clear how two broad peaks separated by 10.3 eV can result from $O_{II}VV$ Auger processes alone. Scheibner and Tharp[21] suggest that the peaks at E = 36.2 and 46.5 eV arise from emission from conduction band states populated by interband excitations associated with the w = 41.5 and 51 eV loses, respectively (resolved at a primary energy of 120 eV). The separation in energy of these two loss peaks is in good agreement with the separation of the secondary peaks, and the loss energies are consistent with excitation

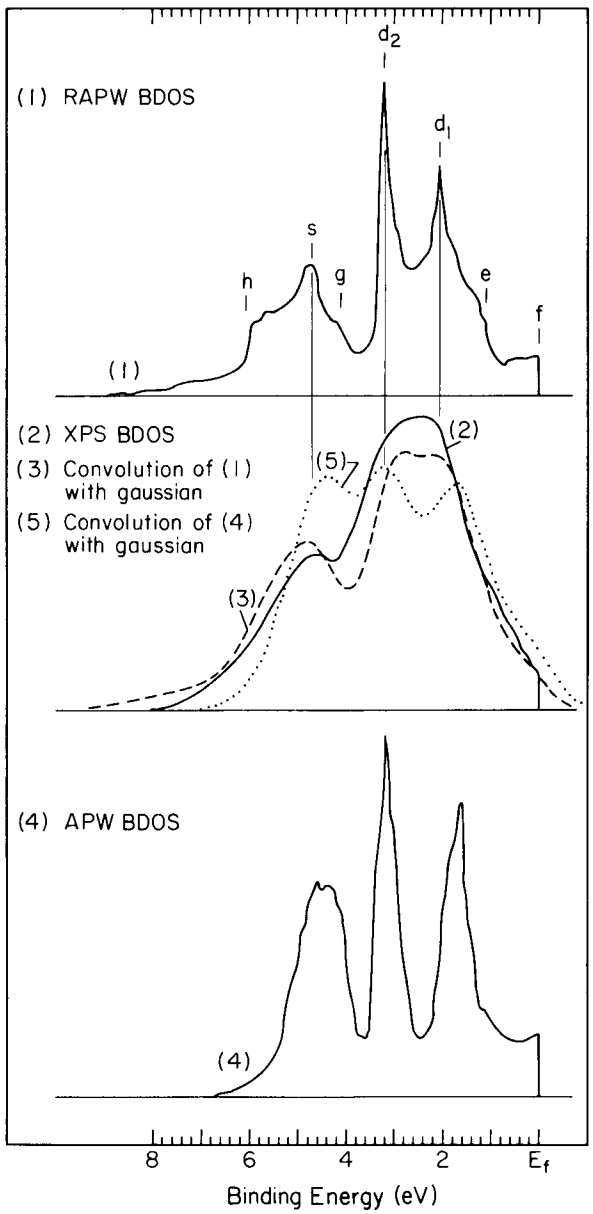

FIG. 2. (1) RAPW valence-band BDOS. The letters above the curve designate features in the BDOS which are associated with structure in the calculated Auger spectra. (2) XPS BDOS obtained from a clean W(111) tungsten crystal.[1] (3) Convolution of curve (1) with a Gaussian with $2\sigma = 0.8$ eV, the width of the Mg $k_{\alpha_{1,2}}$ line. (4) Nonrelativistic BDOS calculation.[23] (5) Convolution of curve (4) with the same Gaussian as used in (3).

of the valence electrons to energy band states at $E = 36.2$ and 46.5 eV. The true secondary peaks at 18.5, 20.3, 21.5, 23.4, 25.6, and 27.6 eV are those which we attribute to *NVV* Auger emission. The structure at 18.5 eV decays when E_p is lowered to 40 eV whereas the shoulder at 16.2 eV resolves itself as a distinct peak, as can be seen by the dotted line in Fig. 1. This different dependence on E_P suggests that these two peaks are of different origin, and we attribute the 16.2-eV peak to energy band states.

Theoretical density of states calculations for tungsten are graphed in Fig. 2. Curve (1) is an RAPW valence-band bulk density of states.[11] The letters above the curve designate features in the BDOS which we associate in the discussion below with structure in the calculated Auger spectra. The two peaks at 2.1 and 3.3 eV, d_1 and d_2 respectively, arise from "d-like" bands. The broad peak at 4.7 eV, s, and shoulders at approximately 4.1 eV, g, and 6.3 eV, h, respectively, are due to bands with "s-like" character. A BDOS spectrum obtained experimentally from a W(111) crystal using XPS is shown as curve (2).[22] An arbitrary linear background has been subtracted. The two "d-like" peaks seen in (1) are not resolved in curve (2). The inherent width of the Mg $k_{\alpha_{1,2}}$ radiation source used to obtain the experimental spectrum is 0.8 eV. If the RAPW calculation, curve (1), is convoluted with a Gaussian with $2\sigma = 0.8$ eV to give curve (3), reasonable agreement between theory and experiment is obtained as can be seen by comparing curves (2) and (3). Curve (4) is the nonrelativistic APW BDOS calculated for tungsten by Mattheiss[23] which was used by Avery[10] in his analysis of *NVV* transitions. This BDOS convoluted with the same Gaussian as used in curve (3) is shown as curve (5). The RAPW calculation appears to offer a better fit to the experimentally measured BDOS in view of the relative intensities of the "s"-

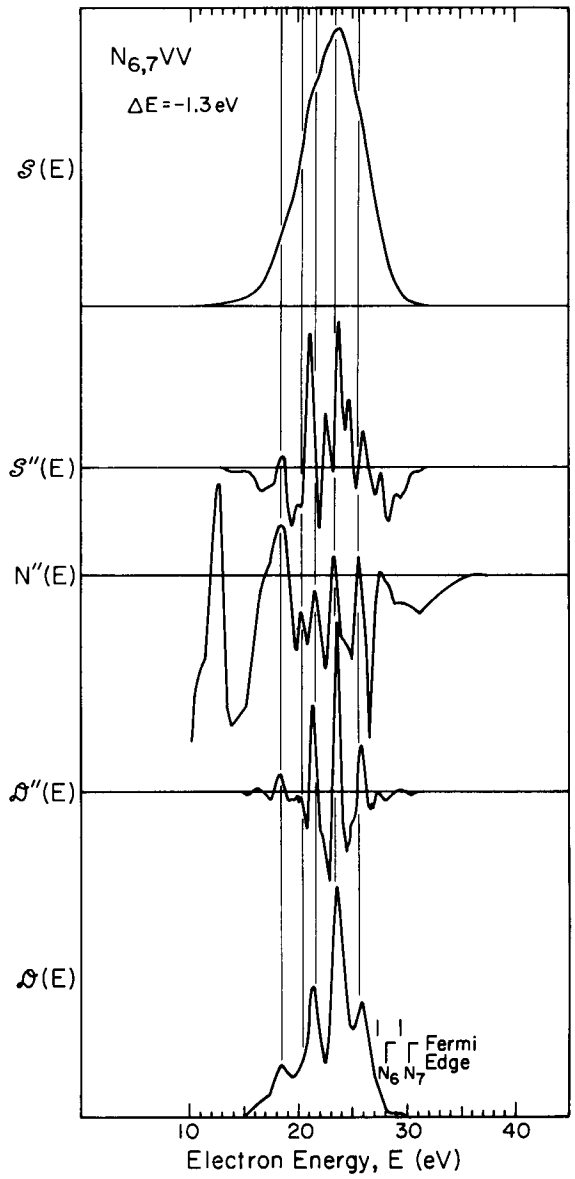

FIG. 3. Comparison of Auger spectrum from clean W(100), $N''(E)$, to the calculated self-convolution, $S''(E)$ and restricted convolution, $D''(E)$ for a model of the Auger process involving both N_6 and N_7 core levels. ΔE for a best fit is taken to be -1.3 eV.

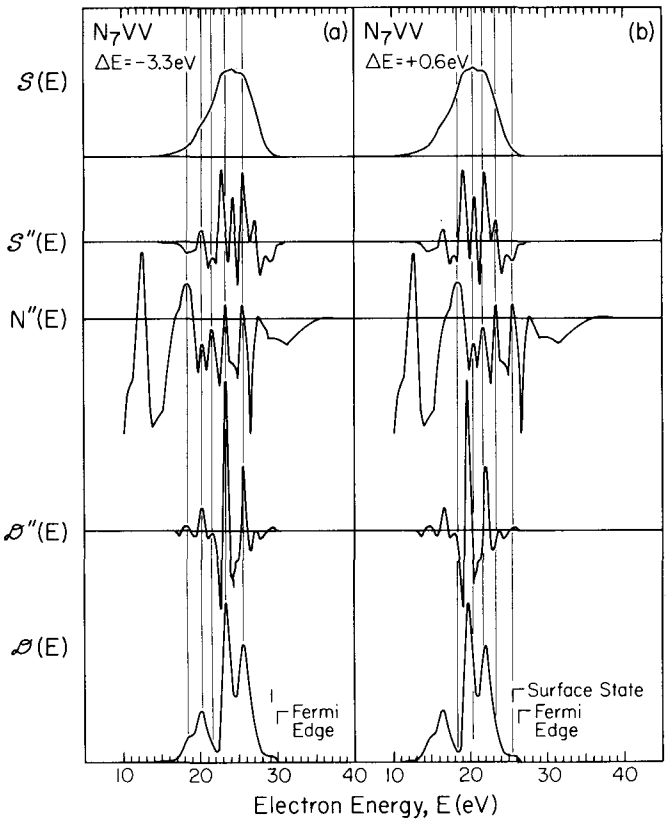

FIG. 4. Comparison of $N''(E)$ to $S''(E)$ and $D''(E)$ for a model of the Auger process (a) involving one core level with $\Delta E = -3.3$ eV and (b) involving one core level plus a surface state for $\Delta E = +0.6$ eV.

and "d"-like states and spacing of the peaks. This calculation has been shown to be consistent with UPS experiments.[18] In evaluating Eqs. (1) and (2) below, $A(\xi)$ and $A(\xi/2)$ were obtained from this RAPW BDOS.

In Figs. 3, 4 and 5, calculations of $D(E)$, $S(E)$, $D''(E) = -d^2D(E)/dE^2$ and $S''(E) = -d^2S(E)/dE^2$ for N_6 or N_7VV and $N_{6,7}$ VV Auger emission for several ΔE values are compared with $N''(E)$ measured for our W(100) surface. We have used values of 31.1, 33.3, and 36.8 eV for the binding energies of the N_6, N_7, and O_{III} core levels. These values were determined with XPS on a well-characterized polycrystalline tungsten surface and include measurements of the valence-band BDOS that allow the authors to determine E_F to within 0.05 eV.[24] Of these models, we propose that $D''(E)$ for $\Delta E = -1.3$ eV shown in Fig. 3 gives the best fit to the experimental data. In the following discussion we present evidence that, within the uncertainties resulting from tungsten's complex electronic structure, this model provides the most reasonable description of the Auger process. Attempts to fit $N''(E)$ with $O_3N_{6,7}VV$ Auger emission failed for both $D''(E)$ and $S''(E)$ regardless of the ΔE chosen. We take this as evidence that O_3VV Auger emission does not contribute significantly to the observed spectrum.

Insight into the origin of the structure in Figs. 3–5 can be obtained by studying the effects of gas adsorption on the Auger spectrum. Second derivative spectra taken after exposure of the clean W(100) surface to hydrogen and oxygen are shown in Fig. 6. Coverage values are not given, but can be related to the given shifts in work function with adsorption, $\Delta\phi$.[16,25] The sensitivity of the features in the Auger spectra to hydrogen and oxygen adsorption have been determined by drawing arbitrary baselines, shown as dotted lines in the clean spectra of Fig. 6, and measuring the peak heights to these baselines. The results are shown in Fig. 7.

For H_2/W(100) the two prominent peaks at 25.6 and 23.4 eV show similar behavior in their coverage dependence although the decrease in the 25.6-eV peak is more pronounced. Both of these peaks reach minimums at $\Delta\phi = 0.18$ eV which corresponds with saturation of the β_2 state (1/4 monolayer).[15] Above 1/4 monolayer, hydrogen adsorbs into the β_1 state. The 21.6-eV peak exhibits similar behavior during filling of the β_2 state. The features in the Auger spectra at 18.5 and 20.5 eV show relatively little change to hydrogen adsorption, although the 18.5-eV peak decreases slightly as hydrogen fills the β_2 state.

Similar results are observed for oxygen adsorption. The 25.6- and 23.4-eV peaks both exhibit a minimum at $\Delta\Phi = 0.27$ eV. This is close to 1/4 monolayer oxygen, the coverage at which the filling of a second bonding state occurs and at which the ESD ion yield from the β_2 state exhibits a maximum.[26] The 21.6-eV peak decreases in intensity for adsorption up to 1/4 monolayer and remains small up to monolayer coverage. The 18.5- and 20.5-eV peaks show little change as in the case of hydrogen adsorption.

The decrease in intensity of the three high energy peaks with adsorption was noted by Avery.[10] He attributed the 25.6-eV structure to an N_7 transition by correlating the decay

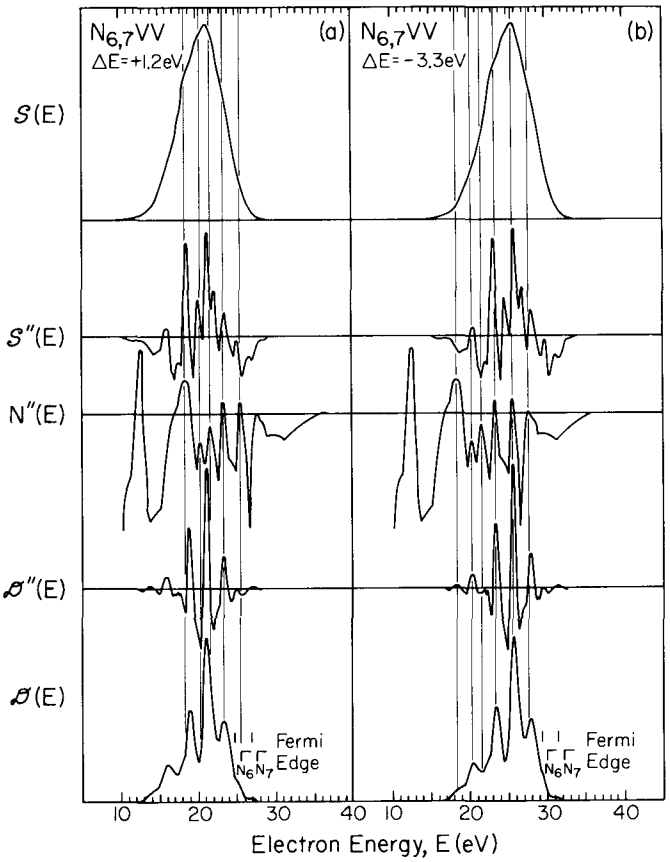

FIG. 5. (a) A best fit of the self-convolution, $S''(E)$, to the experimental Auger spectrum, $N''(E)$ for a model involving both the N_6 and N_7 core levels. (b) Comparison of $N''(E)$ to $S''(E)$ and $D''(E)$ for a model involving two core levels with $\Delta E = -3.3$ eV.

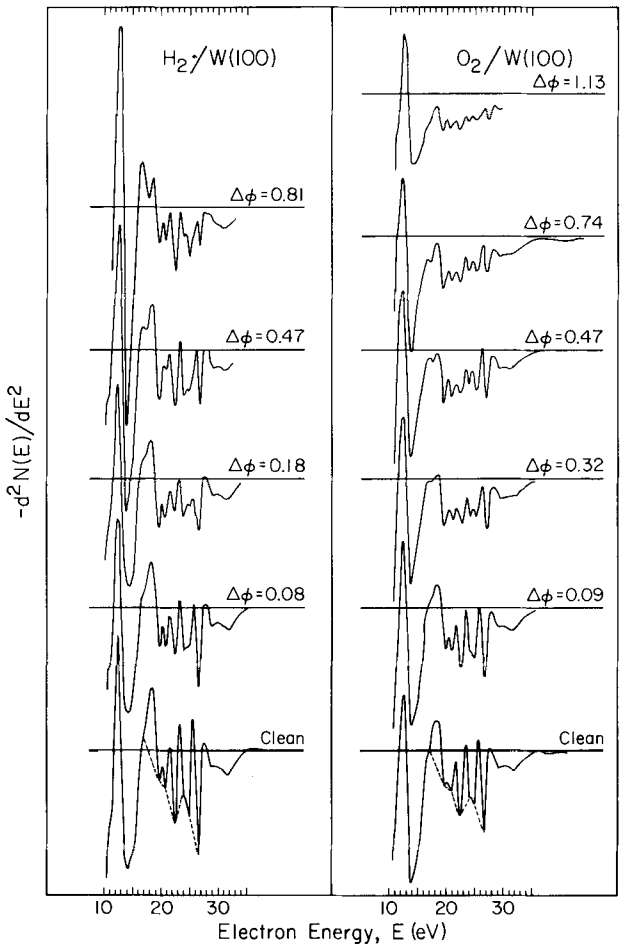

FIG. 6. Change in second derivative of Auger spectrum from W(100) with adsorption of hydrogen (left panel) and oxygen (right panel). Overlayer coverages can be related to the shift in work function, $\Delta\phi$.[16,25] Modulation voltage used was 1 V peak to peak. Hydrogen and oxygen spectra taken at different amplifications.

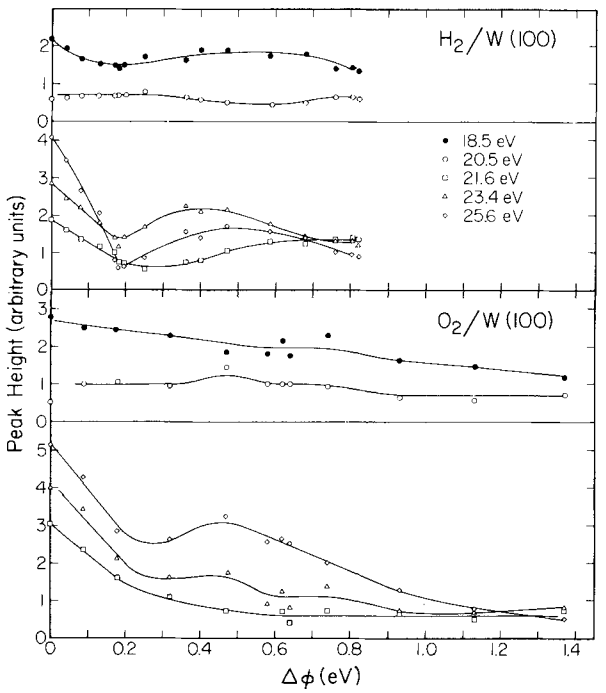

FIG. 7. Change in peak heights of spectra in Fig. 6 with adsorption of hydrogen (top panel) and oxygen (bottom panel).

of this peak to the disappearance of a surface state observed in photoemission and field emission measurements for H_2/W(100).[27-29] In contrast with our results, Avery did not observe structure at 25.6 eV above $\frac{1}{4}$ monolayer. The existence of this peak at coverages where a surface state is not observed suggests that the 25.6-eV peak does not involve surface state transitions. The similar sensitivity of all three high energy peaks to adsorbed hydrogen and oxygen leads us to believe they involve the bonding "*d*-like" electrons in the valence band.

DISCUSSION

The best fit to the experimental data that we obtained is shown in Fig. 3. These calculations assume both N_6VV and N_7VV Auger transitions with $\Delta E = -1.3$ eV and electron populations in the two core states, N_6 and N_7, equal to 3 and 4, respectively. The energy of the peaks in $N''(E)$, $D''(E)$, and $S''(E)$ in Fig. 3 are tabulated in Table I. The column labelled "origins" in this table lists the "*VV*" components of transitions using notation given in Fig. 2. The superscripts label the core level involved in the transition. Note that $D''(E)$ reproduces all of the peaks in $N''(E)$ as well as their energy to within ±0.3 eV. The three narrow, major peaks in $D''(E)$ at 21.4, 23.6, and 25.8 eV all correspond to *d*–*d* excitations $d_2^6d_2^6$, $d_2^7d_2^7$ and $d_1^6d_1^6$, and $d_1^7d_1^7$, respectively. These peaks most strongly resemble the three narrow, major peaks in $N''(E)$ with which they are aligned. The peaks at 18.5 and 20.5 eV in $N''(E)$ correspond to the *s*–*s* excitations s^6s^6 and s^7s^7 in $D''(E)$, respectively. Structure from the h^7h^7 and g^6g^6 shoulders may also contribute to these peaks, respectively. The peaks which we identify in this model as "*d*-like" are strongly perturbed by adsorption as shown in Fig. 7. The states which are "*s*-like" are only weakly perturbed. This is consistent with transition metal chemistry in which bond formation is mostly attributed to *d* orbitals. The 16.2-eV peak in $D''(E)$ arises from the h^6h^6 shoulder and is correspondingly weak. While we attribute the 16.2-eV peak in $N''(E)$ primarily to emission from energy band states, partial contribution to this peak by weak Auger emission is not inconsistant with the experimental data. Structure in $N''(E)$ at 29.5 and 27.6 eV arises from the Fermi

TABLE I. Comparison of energies of structure in $N''(E)$ with energies of structure in $S''(E)$ and $D''(E)$ from Fig. 3. The first column indicates the transitions yielding structure in $D''(E)$ and the last column indicates the transitions yielding structure in $S''(E)$. For $N_{6,7}VV$, $\Delta E = -1.3$ eV.

Origins	$D''(E)$	$N''(E)$	$S''(E)$	Origins
		12.7		
h^6h^6	16.2	16.2	15	h^6*h^6
s^6s^6, h^7h^7	18.3	18.5	18.5	s^6*s^6, h^7*h^7
s^7s^7, g^6g^6	20.2	20.5	20.1	s^7*s^7, $s^6*d_2^6$, $d_2^6*s^6$, g^6*g^6
$d_2^6d_2^6$	21.4	21.6	21.1	$d_2^6*d_2^6$, $d_1^6*s^6/s^6*d_1^6$
			22.6	$d_2^6*d_1^6/d_1^6*d_2^6$
$d_2^7d_2^7$, $d_1^6d_1^6$	23.6	23.4	23.8	$d_2^7*d_2^7$, $d_1^6*d_1^6$, $d_1^7*s^7/s^7*d_1^7$
			24.7	$d_2^7*d_1^7/d_1^7*d_2^7$
$d_1^7d_1^7$	25.8	25.6	26.0	$d_1^7*d_1^7$
e^7e^7, f^6f^6	27.4	27.6	27.7	e^7*e^7, f^6*f^6
f^7f^7	29.4	29.5	29.0	f^7*e^7/e^7*f^7
			30.6	f^7*f^7

edge, f, and from the prominent increase in the BDOS at e as shown in Table I. These peaks also do not follow the behavior of the d–d peaks with adsorption.

A narrow surface state, which is strongly attenuated by adsorption, has been observed 0.4 eV below E_F on W(100) by field emission and UPS.[26–28] If surface state emission involving the N_6 and N_7 core levels ($N_{6,744}$) occurs, well defined peaks should be observed at 27.3 and 29.5 eV in $N''(E)$ in Fig. 3. No evidence for $N_{6,744}$ emission exists in this model: the hump at 29.5 eV in $N''(E)$ is broad and both it and the 27.6-eV peak are very insensitive to surface chemistry.

The most significant difference which exists between $S''(E)$ and $D''(E)$ in Fig. 3 is the absence in $D''(E)$ of the $d_2^6 * d_1^6/d_1^6 * d_2^6$ cross-term peak at 22.6 eV and the $d_2^7 * d_1^7/d_1^7 * d_2^7$ cross-term peak at 24.7 eV. The good agreement with $N''(E)$ which $D''(E)$ exhibits therefore suggests that the matrix elements for Auger emission from W(100) are much larger when both "up" and "down" electrons associated with the s, d_1, and d_2 peaks in the BDOS originate at the same or nearly the same energy. The reason for this result is not known. However, the cross term matrix elements would be small if, for example, the two "d-like" peaks have primarily e_g and t_{2g} symmetry, respectively. Such a condition occurs in some metals, including silver.[4] Two results, however, remain to be explained. No mechanism emerges from this model to generate the shoulder at ~24.5 eV. In addition, the even spacing between the three main peaks at 21.4, 23.6, and 25.8 eV inherent in the calculated spectra is lacking in the experimental spectra. While this difference between the calculation and experiment is small, it is quite reproducible and appears real.

Fig. 4(a) describes a model for N_7VV Auger emission for $\Delta E = -3.3$ eV. For the self-convolution, $S''(E)$, to represent a reasonable description of $N''(E)$, the $d_1 * d_2/d_2 * d_1$ cross terms must be strongly attenuated while $s * d_2/d_2 * s$ transitions must be strongly enhanced. In addition, h–h emission peaking at the bottom of the band must be invoked to explain the absence of the 18.5 eV peak in $S''(E)$. The attenuated cross term peak provides an explanation for the origin of the shoulder in $N''(E)$ between the 23.4- and 25.6-eV peaks. This is the only model we found that offers an explanation for this shoulder. With the above assumptions, $S''(E)$ provides an acceptable agreement with $N''(E)$ for a single core level model for the Auger data.

Only for N_7VV plus N_{744} Auger emission with $\Delta E = +0.6$ eV could we approach fitting $S''(E)$ to $N''(E)$ without eliminating at least one cross-term peak. While this model, shown in Fig. 4(b) is basically equivalent to the model employed by Avery, the origins of the peaks in $N''(E)$ are different from Avery's due to the significant differences in the BDOS used. Figure 4(b) attributes the 23.4 eV peak in $N''(E)$ to $e * e$ emission ($d_1 * d_1$ in Avery's work), the 21.6 eV peak to $d_1 * d_1$ emission ($d_1 * d_2/d_2 * d_1$ in Avery's work) and the 20.5-eV peak to $d_1 * d_2/d_2 * d_1$ emission ($d_2 * d_2$; $d_1 * s/s * d_1$ in Avery's work). This lack of agreement in peak origins illustrates the critical dependence of this analysis on accurate knowledge of the BDOS.

As was done by Avery, we aligned the energy at which N_{744} Auger emission would be predicted in $-S''(E)$ with the 25.6 eV peak in $N''(E)$. However, our demonstration in Fig. 7 that major differences do not exist in the chemical effects on the three major peaks in $N''(E)$ makes this assignment a highly arbitrary one. It is also not *a priori* obvious that N_6 holes are effectively annihilated by Coster–Kronig transitions involving N_7 electrons as proposed by Avery; in particular, no evidence of lifetime broadening of the N_6 tungsten core level by Coster–Kronig transitions is observed in XPS[22] and ELS[16] and contributions from both N_6 and N_7 core levels have been observed in the NVV spectrum of gold.[30]

A "best" fit of $S''(E)$ to $N''(E)$ for $N_{6,7}VV$ Auger emission is obtained with $\Delta E = 1.2$ eV. This is shown in Fig. 5(a). The inclusion of both N core levels identifies the peak at 25.6 eV in $N''(E)$ with $e^7 * e^7$, $f^6 * f^6$ Auger emission and removes the necessity of invoking surface state Auger emission. However, the $d_2^7 * d_1^7/d_1^7 * d_2^7$ cross-term peak in $S''(E)$ is absent in $N''(E)$ while the $d_2^6 * d_1^6/d_1^6 * d_2^6$ peak is associated with the shoulder at 20.4 eV in $N''(E)$, a dilemma which basically eliminates this model from consideration. $D''(E)$ demonstrates that elimination of both cross-term peaks does not improve the model.

Fig. 5(b) gives another comparison of measured and calculated $N_{6,7}VV$ spectra for $\Delta E = -3.3$ eV. In this comparison, $D''(E)$ does not reproduce the shape and strength of the 21.6 eV peak in $N''(E)$ particularly well. Furthermore, in contrast with our experiments, this model predicts that the chemical behavior of this peak should resemble that of the 20.5 eV peak since both arise from s-like emission. Only by invoking $s^6 * d_2^6$ cross-term peaks can this be rationalized. Similarly, this model also predicts that the 25.6 and 27.6 eV peaks should exhibit similar chemistry dependences which is not observed. The large negative value of ΔE is also weighed against the validity of this model.

CONCLUSIONS

We have analyzed the CVV Auger spectrum from W(100) using two models of the Auger process: one in which all possible "up" and "down" transitions are uniformly probable across the valence band, and one in which all "up" and "down" transitions are uniformly probable, but with the restriction that both electrons involved in an Auger transition originate at the same valence energy. The complexity of tungsten's electronic structure limits the effectiveness of these simple models in providing a definitive description of the CVV Auger spectrum. A number of conclusions and observations can, however, be drawn from this analysis:

(1) An accurate knowledge of the energy band structure is extremely important in deriving an unambiguous description of even the most basic features of tungsten's CVV Auger spectrum.

(2) Strong variations in the Auger transition matrix elements occur across the valence band. The assumption of uniform up and down transition probability across the valence band is not valid.

(3) Prominent structure in the CVV Auger spectrum does not arise from electrons localized in the W(100) surface resonance.

(4) Appreciable Coster–Kronig annilation of the N_6 hole as proposed by Avery is not observed.

(5) The best agreement between our calculated Auger spectra and the experimental measurements exists for an $N_{6,7}VV$ Auger model in which cross terms between different energy states are neglected. This model reproduces all the prominent peak energies within ±0.3 eV and gives reasonable agreement with peak shapes. Furthermore, the origins ascribed to the peaks are consistent with observed chemical effects exhibited upon adsorption.

ACKNOWLEDGMENTS

The authors would like to express their appreciation to the staff of the Coordinated Science Laboratory for their support in the experimental phases of this work and to Dr. S. L. Cunningham for help in computation. This work was supported in part by the Joint Services Electronics Program (U.S. Army, Navy, and Air Force) under contract DAAB 07-72-C-0259.

[a]Present address: Solid State Division, Oak Ridge National Laboratory, Oak Ridge, TN 37830.
[b]Present address: Varian Associates, Palo Alto, CA.
[c]Present address: CERL, University of Illinois, Urbana, IL 61801.
[d]Alfred P. Sloan Foundation Fellow, and Camille and Henry Dreyfus Teacher-Scholar.

[1]G. F. Amelio, Surf. Sci. **22,** 301 (1970); P. J. Feibelman, E. J. McGuire, and K. C. Pandey, Phys. Rev. Lett. **36,** 1154 (1976); R. G. Musket and R. J. Fortner, Phys. Rev. Lett. **26,** 80 (1971); J. Tejeda, N. J. Shevchik, D. W. Langer, and M. Cardona, Phys. Rev. Lett. **30,** 370 (1973); and J. E. Houston, J. Vac. Sci. Technol. **12,** 255 (1975).
[2]J. J. Lander, Phys. Rev. **91,** 1382 (1953).
[3]C. J. Powell, Phys. Rev. Lett. **30,** 1179 (1973).
[4]James M. Burkstrand and Gary G. Tibbetts, Phys. Rev. B **15,** 5481 (1977).
[5]P. J. Feibelman, E. J. McGuire, and K. C. Pandey, Phys. Rev. Lett. **36,** 1154 (1976).
[6]L. Yin, I. Adler, T. Tsang, M. M. Chen, and B. Crasemann, Phys. Lett. A **46,** 113 (1973).
[7]A. M. Baro, M. Salmeron, and J. M. Rojo, J. Phys. F **5,** 826 (1975).
[8]J. E. Houston and M. G. Lagally, J. Vac. Sci. Technol. **13,** 361 (1976).
[9]P. J. Bassett, T. E. Gallon, J. A. D. Matthew, and I. Prutton, Surf. Sci. **35,** 63 (1973).
[10]N. R. Avery, Surf. Sci. **61,** 391 (1976);
N. R. Avery, Phys. Rev. Lett. **32,** 1248 (1974).
[11]N. E. Christensen and B. Feuerbacher, Phys. Rev. B **10,** 2349 (1974).
[12]P. E. Luscher, S. P. Withrow, and F. M. Propst (in preparation).
[13]J. F. Wendelken, S. P. Withrow, and C. A. Foster, Rev. Sci. Instrum. **48,** 1215 (1977).
[14]D. R. Sandstrum and S. P. Withrow, J. Vac. Sci. Technol. **14,** 748 (1977).
[15]S. P. Withrow, Ph.D. thesis, Univ. of Ill. (1975) (unpublished).
[16]P. E. Luscher, Surf. Sci. **66,** 157 (1977).
[17]While loss structure with energies as large as 70 eV have been observed, (Ref. 16) contributions with loss energies >50 eV are negligible in Fig. 1.
[18]B. Feuerbacher and N. E. Christensen, Phys. Rev. B **10,** 2373 (1974).
[19]P. W. Palmberg, G. E. Riach, R. E. Weber, and N. C. MacDonald, *Handbook of Auger Electron Spectroscopy* (Physical Electronics Industries, Inc., Edina, MN, 1972), p. 139.
[20]K. Seigbahn, C. Nordling, A. Fahlman, R. Nordberg, K. Hamrin, J. Hedman, G. Johansson, T. Bergmark, S.-E. Karlsson, I. Lindgren, and B. Lindberg, in *ESCA-Atomic, Molecular, and Solid State Structure Studied by Means of Electron Spectroscopy,* (Almquist and Wiksells, Uppsala, 1967).
[21]E. J. Scheibner and L. N. Tharp, Surf. Sci. 8 247 (1967).
[22]J. T. Yates, Jr., and N. Erickson, Surf. Sci. **44,** 489 (1974).
[23]L. F. Mattheiss, Phys. Rev. **139,** 1893 (1965).
[24]J. T. Yates, Jr., T. E. Madey, and N. Erickson, Surf. Sci. **43,** 257 (1974).
[25]T. E. Madey and J. T. Yates, Jr., Structure et Propriétés des Surfaces des Solides (Editions du Centre National de la Recherche Scientifique, Paris, 1970) No. 187, p. 155.
[26]Paul E. Luscher and F. M. Propst, J. Vac. Sci. Technol. **14,** 400 (1977).
[27]B. J. Waclawski and E. W. Plummer, Phys. Rev. Lett. **29,** 783 (1972).
[28]E. W. Plummer and J. W. Gadzuk, Phys. Rev. Lett. **25,** 1493 (1970).
[29]B. Feuerbacher and B. Fitton, Phys. Rev. Lett. **29,** 786 (1972).
[30]C. J. Powell (unpublished).